



Network Pharmacology-Based Prediction of the Mechanism of Anti-Hepatitis C Virus of *Kleinhovia hospita* L

Muhammad Arba^{1*}, Sunandar Ihsan¹, Milba N. Mazida¹, Jamili Jamili², Tutik S. Wahyuni³¹Department of Pharmaceutical Analysis and Medicinal Chemistry, Faculty of Pharmacy, Universitas Halu Oleo, Kendari, Indonesia²Department of Biology, Faculty of Science, Universitas Halu Oleo, Kendari, Indonesia³Department of Pharmaceutical Science, Faculty of Pharmacy, Universitas Airlangga, Indonesia

ARTICLE INFO

Article history:

Received 24 July 2025

Revised 08 August 2025

Accepted 20 August 2025

Published online 01 October 2025

ABSTRACT

Copyright: © 2025 Arba *et al.* This is an open-access article distributed under the terms of the [Creative Commons Attribution License](#), which permits unrestricted use, distribution, and reproduction in any medium, provided the original author and source are credited.

Kleinhovia hospita L. is tropical herbaceous plant typically used as traditional medicine, but its potential as an antiviral agent remains scientifically underexplored. Given the limitations of the current hepatitis C virus (HCV) treatments, there is a need to identify novel therapeutic compounds from natural resources. Therefore, this study aims to explore the potential of the methanol extract of *Kleinhovia hospita* L. to treat HCV. Chemical composition of the methanol extract was assessed using liquid chromatography-high-resolution mass spectrometry (LC-HRMS). The protein targets and signaling pathways in HCV due to *Kleinhovia hospita* L. were evaluated with network pharmacology. Computational results were then validated using *in vitro* testing against HCV. The LC-HRMS analysis results showed that there were 57 compounds in the methanol extract, with 38 complying with drug-likeness properties. Network pharmacology analysis using the 38 compounds showed 331 potential therapeutic targets, with TP53, AKT1, SRC, HSP90AA1, EGFR, GAPDH, and ESR1 serving as core targets. Molecular docking of the best 4 targets (TP53, AKT1, SRC, HSP90AA1) showed that the AKT1-bound docked poses of Compounds 2, 7, 11, 20, 24, 33, 38, 43, and 45 had lower binding energies than native ligand. Meanwhile, compounds 28 and 40 showed lower binding energies than the native ligand when bound to SRC. Lower binding energies were also observed in the HSP90-docked poses of compounds 7, 24, 25, and 55. *In vitro* test against HCV by the methanol extract showed inhibitory concentration 50 (IC₅₀) of 2.24±0.1 µg/mL, which indicated its potential for inhibiting HCV.

Keywords: Hepatitis C, *Kleinhovia hospita*, Network pharmacology, Herbal plant, *in vitro* test

Introduction

Hepatitis C virus (HCV) is a lipid-enveloped, positive-strand RNA virus with a genome of roughly 9.6 kb, belonging to the *Flaviviridae* family and the *Hepacivirus* genus. Persistent HCV infection is a major etiological factor for the chronic liver diseases, most notably hepatocellular carcinoma (HCC).¹⁻² According to the World Health Organization (WHO), approximately 1.5 million new infections occur annually, with an estimated 290,000 deaths and nearly 58 million individuals living with HCV worldwide.³⁻⁵ These global epidemiological figures highlight the pressing necessity for more effective and innovative therapeutic strategies against HCV.

A tropical herbaceous plant, *Kleinhovia hospita* L., was reported to have several pharmacological activities. For instance, Arung *et al.* 2009 reported the strong antioxidant activity of *Kleinhovia hospita* leaf extracts and moderate cytotoxicity.⁶ Arieftha *et al.* (2024) showed that the extract from the plant showed antiparasmodial activity against *Plasmodium falciparum* strains 3D7 and K1.⁷ Solihah (2019) reported that its ethanol extract had the most potential as a cytotoxic agent, which could be relevant for further studies in areas such as cancer treatment.⁸ Despite the potential of the plant, there are no studies regarding its activity against HCV.

*Corresponding author. E mail: muh.arba@uho.ac.id

Tel: +628114056877

Citation: Arba M, Ihsan S, Mazida MN, Jamili J, Wahyuni TS. Network Pharmacology-Based Prediction of the Mechanism of Anti-Hepatitis C Virus of *Kleinhovia Hospita* L. Trop J Nat Prod Res. 2025; 9(9): 4460 – 4467 <https://doi.org/10.26538/tjnpr/v9i9.46>

Official Journal of Natural Product Research Group, Faculty of Pharmacy, University of Benin, Benin City, Nigeria

Therefore, this research seeks to investigate the potential of the methanol extract of *Kleinhovia hospita* L. to treat HCV using network pharmacology, molecular docking, and *in vitro* assessment. Network pharmacology is an emerging interdisciplinary field that merges concepts from biology, pharmacology, and informatics.⁹⁻¹⁰ It is particularly well-suited to uncover the synergistic effects of herbal plants, which typically consist of multiple active compounds working through various targets and pathways to produce therapeutic outcomes. This approach enables the mapping of interactions between compounds and their biological targets, making it a powerful tool for exploring the pharmacological basis of herbal plants.¹¹ As it remains a theoretical framework, integrating it with *in vitro* study can help substantiate these predictions and clarify how herbal plant exerts therapeutic effects. Here we applied network pharmacology, molecular docking, and *in vitro* studies to explore the anti-HCV mechanisms of *Kleinhovia hospita* L. methanol extract.

Materials and methods

Plant sample preparation and extraction method

Kleinhovia hospita L. leaves were taken in June 2024 from Forest Management Unit (FMI) Gantara, Liwu Metingki village, Muna District, Southeast Sulawesi, Indonesia. The Gantara FMI was located south of the equator, from 04°43'58.52" South Latitude (SL) to 05°07'30.06" South Latitude (SL), and from 122°46'09.08" East Longitude (EL) to 122°56'44.85" East Longitude (EL). Identification of the plant was performed by the Laboratory of Pharmacy, Universitas Halu Oleo, Indonesia, under registration number 1704/UN29.18.1.1/PP/2025 and specimen code FF-UHO-066. In addition, the leaves of the plant were wet-sorted, washed, cut into thin slices, and then air-dried. The crude simplisia of *Kleinhovia hospita* L. (1.5 kg) was subsequently subjected to maceration with methanol (15

L) for 3 x 24 hours, followed by evaporation to obtain a 130.45 g crude extract.

LC-HRMS analysis

The chemical constituents of the crude extract of *Kleinhovia hospita* L. leaf were investigated by liquid chromatography-high resolution mass spectrometry (LC-HRMS).¹²⁻¹³ Chromatographic separation was performed using a Thermo Scientific™ Vanquish™ UHPLC Binary Pump system, integrated with a Thermo Scientific™ Q Exactive™ Hybrid Quadrupole-Orbitrap™, High-Resolution Mass Spectrometer. A Thermo Scientific™ Accucore™ Phenyl-Hexyl column (100 mm × 2.1 mm ID × 2.6 µm) was used for the analysis, with all procedures and conditions and the specific conditions and procedures conducted according to a previously reported method.¹⁴

In silico analysis

Compounds obtained from LC-HRMS analysis were subjected to drug-likeness prediction using the SwissADME web server (<http://www.swissadme.ch/>).¹⁵ The Lipinsky rule of 5, bioavailability scored > 0.55, and high gastrointestinal absorption, were used as screening criteria. Compounds violating the Lipinsky rule of 5 more than a criterion, and or had a bioavailability score < 0.55, and low gastrointestinal absorption were left from subsequent study.

Target screening

The target prediction for the methanol extract of *Kleinhovia hospita* L. was carried out using the SwissTargetPrediction and SEA (<https://sea.bkslab.org>) databases,¹⁶⁻¹⁷ while HCV-related genes were predicted using OMIM (<https://www.omim.org>) and GeneCard (<https://www.genecards.org>) databases,¹⁸⁻²⁰ and were then refined by selecting the top 500 targets.²¹ Finally, the predicted targets from the compounds and the disease-associated genes were compared and visualized using a Venn diagram created with the Bioinformatics and Systems Biology tool (<https://bioinformatics.psb.ugent.be/webtools/Venn/>).

Protein-Protein Interaction (PPI) Network

String Database (<https://string-db.org>) was used to construct PPI using common targets as an input, in which the protein target was limited to the species "*Homo sapiens*" and high confidence 0.007. Subsequently, the PPI network was obtained using Cytoscape v3.10.2.²²

Gene ontology (GO) analysis and KEGG pathway

GO analysis was performed using the Metascape (<https://www.metascape.org>) and shinyGO 0.80 databases to assess the biological functions, cellular processes, and molecular components associated with the predicted protein targets.²³⁻²⁵ Additionally, KEGG (Kyoto Encyclopedia of Genes and Genomes) pathway analysis was used to identify metabolic pathways and molecular signaling routes influenced by the active compounds and target proteins of *Kleinhovia hospita* L. and HCV. The identified pathways were regarded as the potential mechanisms through which the compounds exerted their effects.

Molecular Docking

Molecular docking was performed on the 4 best targets to evaluate the binding mode and affinity of the compound to a receptor target, which meant tumor suppressor protein 53 (TP53), AKT serine/threonine kinase 1 (AKT1), sarcoma (SRC), and heat shock protein (HSP90AA1). All PDB structure files of each protein target were downloaded from the Protein Data Bank database (<https://www.rcsb.org>).

The 2-dimensional structures of the compound identified through LC-HRMS of the methanol extract of *Kleinhovia hospita* L. were built into 3D forms using the Maestro LigPrep module with the OPLS_2005 force field.²⁶⁻²⁷ Preparation of both proteins and ligands followed established protocols,²⁸ using the Maestro Schrödinger software version 11.1.012, release 2017-1 (Schrödinger, New York, NY, USA).²⁹ Grid points were

set up following the position of each native ligand of TP53, AKT1, SRC, and HSP90AA1.

Cell culture, virus preparation, and anti-HCV activity

This study used cloned human liver cancer cell lines (Huh7it-1).³⁰ The culture medium consisted of DMEM enriched with additional amino acids, 10% fetal bovine serum (Biowest), and kanamycin (Sigma-Aldrich). Incubation was carried out at 37 °C in a 5% CO₂ atmosphere, and the HCV strain used in the experiments was JFH-1, which belonged to genotype 2a.³¹ Antiviral testing was carried out according to the previously protocol.³¹ Cells were exposed with the virus at a multiplicity of infection (MOI) of 0.1 and treated by varying concentrations (0.01, 0.1, 1, 10, 50, and 100 µg/mL) of methanol extract of *Kleinhovia hospita* L. leaves. Following a 2-hour incubation at 37 °C, the viral solution was removed, and the cells were maintained with the extract for an additional 46 hours at the same temperature. Culture supernatants were then collected to evaluate viral levels, based on the procedure described by Apriyanto and colleagues (36), and the IC₅₀ value was calculated using probit analysis with SPSS software.³²

Results and Discussion

Identification of active compounds and target prediction

A total of fifty-seven bioactive compounds were identified by LC-HRMS on the methanol extract of *Kleinhovia hospita* L (Table S1). Analysis of drug-likeness using Lipinsky rule of 5, bioavailability score and gastrointestinal absorption criteria found out 19 compounds did not pass the criteria, which meant Compound 1, 3, 4, 6, 8, 14, 15, 17, 18, 19, 21, 22, 30, 36, 37, 46, 47, 51, and 52 (Table S2). Therefore, only 38 compounds were processed for further analysis. As many as 5281 and 2274 potential targets of *Kleinhovia hospita* L. were predicted through SwissTargetPrediction and SEA databases, respectively, while 375, 503, and 270 gene targets for HCV were predicted by OMIM, GeneCard, and DisGenet databases, respectively. A total of 331 HCV-related targets were identified at the intersection and were selected as hub genes between *Kleinhovia hospita* L. targets and those correlated with HCV, as shown in the Venn diagram (Figure 1).

Construction of compound-target network analysis

Based on the 331 targets above, the relationship between bioactive compounds of the methanol extract of *Kleinhovia hospita* L. and the therapeutic target of HCV was showed. These targets were then entered into the STRING database to retrieve PPI network data, and the results were visualized using Cytoscape software. The compound-target network was composed of 331 nodes and 2105 edges. In this network, nodes represented the target genes and their associated compounds, while the edges showed the interactions between these nodes (Figure 2). From the 331 nodes, the top 10, based on their degree values, were selected as the hub key targets. These hub nodes could be crucial within the PPI network in mediating anti-HCV effects. Details of the top 10 nodes, including their corresponding closeness centrality and betweenness centrality, were provided in Table 1.

The degree value represented how many associations were predicted between each component and its corresponding targets. A higher degree suggested that the component played a more significant role. Furthermore, it was found that those targets having higher degree included tumor protein 53 (TP53), RAC-alpha serine/threonine protein kinases 1 (AKT1), sarcoma (SRC), heat shock protein 90 (HSP90AA1), epidermal growth factor receptor (EGFR), B-cell lymphoma 2 (BCL2), glyceraldehyde-3-phosphate dehydrogenase (GADPH2), nuclear factor kappa B subunit 1 (NFKB1), jun proto-oncogene (JUN), and estrogen receptor (ESR1), and taken as hub key targets. Closeness centrality reflected how centrally located a node was, and betweenness centrality highlighted nodes that served as key connectors or bridges within the network.³³

The top 10 proteins from each centrality measure identified were further analyzed using a Venn diagram. This analysis showed 7 overlapping proteins— TP53, AKT1, SRC, HSP90AA1, EGFR, GAPDH, ESR1— which were proposed as key targets. Figure 3 showed the top 10

potential target proteins were identified based on the highest scores across different centrality measures, namely (a) degree, (b) betweenness, and (c) closeness. A Venn diagram showed the overlap

among these top proteins, highlighting 7 key targets which included TP53, AKT1, SRC, HSP90AA1, EGFR, GAPDH, and ESR1.

Table 1: Top ten targets with their degree, closeness centrality, and betweenness centrality values.

Name	Degree	Betweenness centrality	Closeness centrality
TP53	94	0.1141376743448232	0.5098684210526316
AKT1	79	0.052046117435341856	0.5008077544426495
SRC	75	0.06656047482218538	0.48665620094191525
HSP90AA1	73	0.04779635699227042	0.47473200612557426
EGFR	72	0.06173529812557463	0.496
BCL2	62	0.036966958063187234	0.4718417047184171
GAPDH	55	0.051338004893963986	0.484375
NFKB1	54	0.016129244598454683	0.45454545454545453
JUN	53	0.023945572004196034	0.4661654135338346
ESR1	52	0.04745410010432503	0.4682779456193354

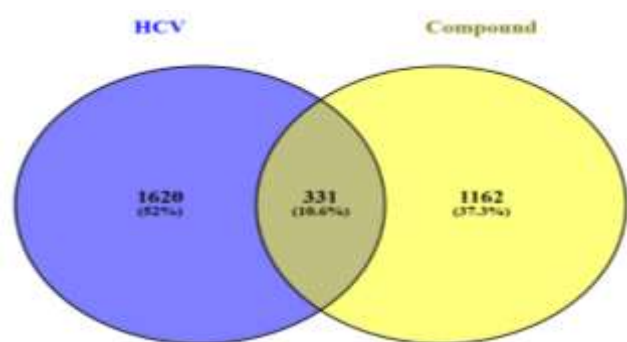


Figure 1: Venn diagram of the common target of hepatitis C virus- *Kleinhovia hospita* L. Blue indicated genes of hepatitis C virus, yellow indicated targets of compounds of *Kleinhovia hospita* L., and light yellow indicated the common target.

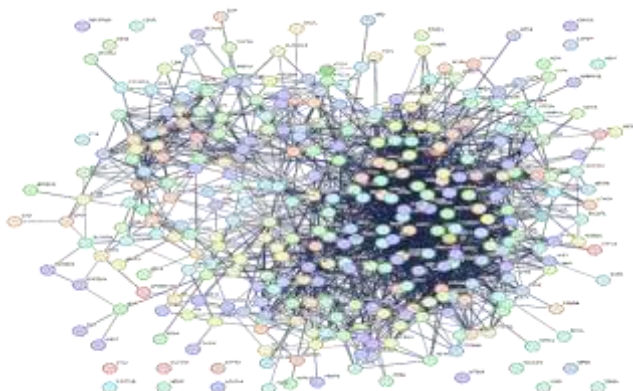


Figure 2: The interactive PPI network was generated using the STRING database, which consisted of 331 nodes and 2105

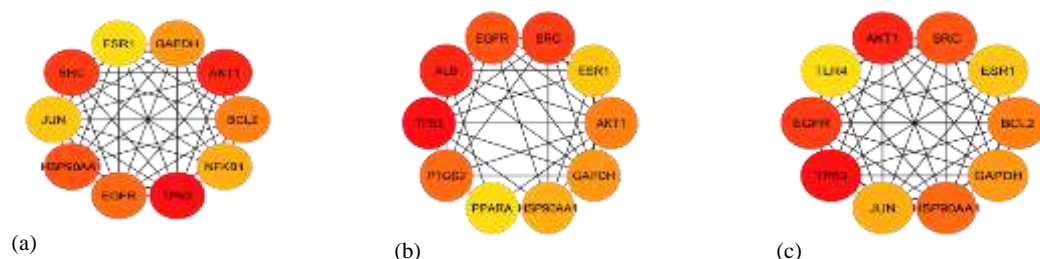
edges. Each node corresponds to a potential target, while the edges represent various types of protein-protein interactions. These include known interactions (azure for curated databases and purple for experimental evidence), predicted interactions (green for gene neighborhood, red for gene fusions, and blue for gene co-occurrence), and additional associations (light green for text mining, black for co-expression, and light blue for protein homology).

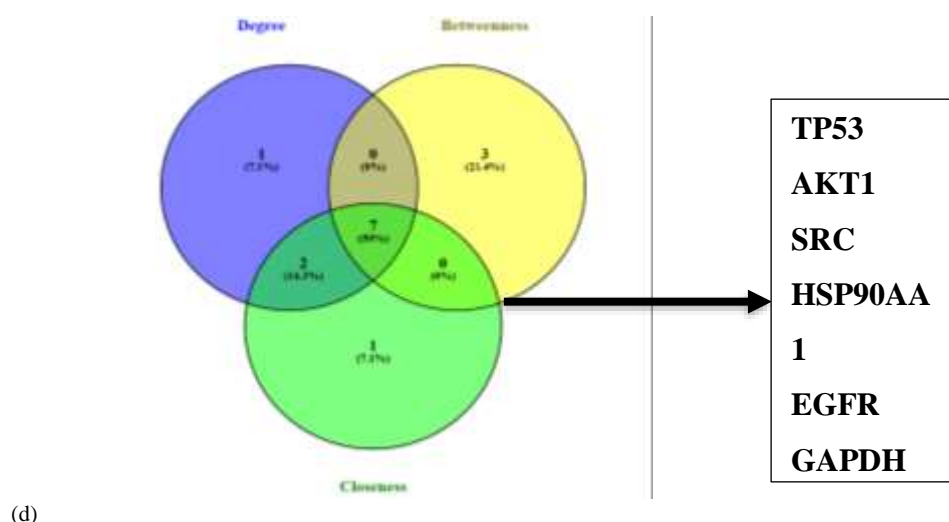
GO enrichment and KEGG pathway analysis

The 331 intersecting targets were further analyzed to show the mechanism of action of their anti-HCV activity using GO and KEGG pathway enrichment analysis using shiny GO 0.80, to elucidate the functions and pathways of genes in HCV. These two pathways were analyzed in terms of biological process (BP), cellular components (CC), and molecular function (MF), and a total of 1000 GO BP, 301 GO CC, 793 GO MF, and 257 KEGG pathways were enriched.

The top 10 enrichments of GO BP showed that the target genes of the methanol extract of *Kleinhovia hospita* L. associated with response to chemical, [cellular response to chemical stimulus](#), [response to organic substance](#), [response to oxygen-containing compound](#), and [cellular response to organic substance](#). The target genes were mainly found in the [receptor complex](#), [cell surface](#), [vesicle](#), [membrane raft](#), and [membrane microdomain](#), as shown by the GO CC. These MF showed that the target genes were mainly involved in protein kinase activity, phosphotransferase activity, alcohol group as acceptor, kinase activity, protein serine/threonine/tyrosine kinase activity, and identical protein binding.

Substantial signaling pathways related to HCV were analysed by KEGG pathway, which showed that the effect of *Kleinhovia hospita* L. in treating HCV was associated with [pathways in cancer](#), [lipid and atherosclerosis](#), [kaposi sarcoma-associated herpesvirus infection](#), [hepatitis B](#), and [PI3K-Akt signaling pathway](#). Furthermore, Figure 4 showed the bubble map of the top signification GO terms and KEGG pathways.





(d)

Figure 3: The top 10 potential target proteins identified based on (a) degree (b) betweenness (c) closeness. Seven key targets: TP53, AKT1, SRC, HSP90AA1, EGFR, GAPDH, ESR1 overlap among top ten proteins (d).

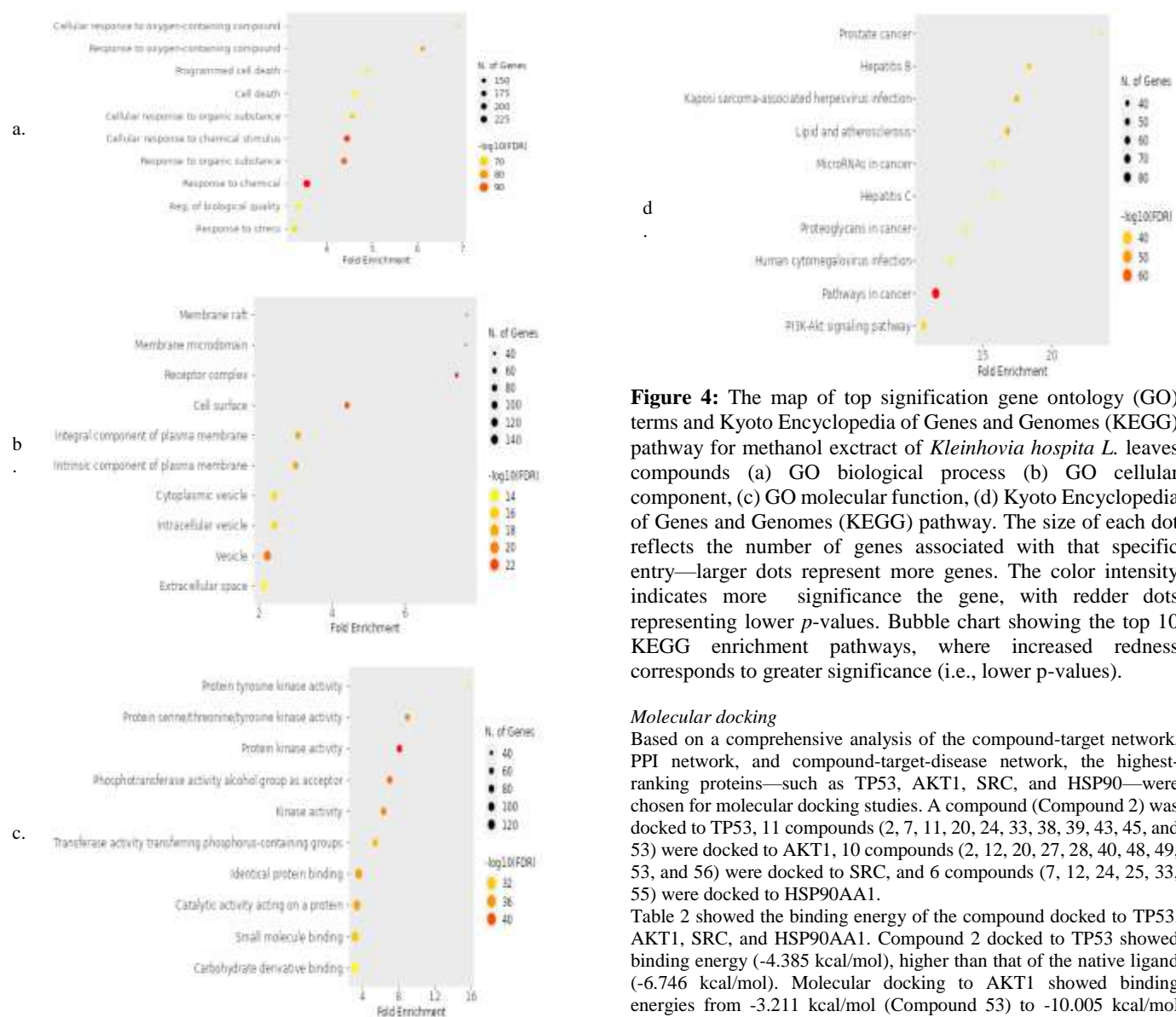


Figure 4: The map of top significant gene ontology (GO) terms and Kyoto Encyclopedia of Genes and Genomes (KEGG) pathway for methanol extract of *Kleinhovia hospita* L. leaves compounds (a) GO biological process (b) GO cellular component, (c) GO molecular function, (d) Kyoto Encyclopedia of Genes and Genomes (KEGG) pathway. The size of each dot reflects the number of genes associated with that specific entry—larger dots represent more genes. The color intensity indicates more significance the gene, with redder dots representing lower *p*-values. Bubble chart showing the top 10 KEGG enrichment pathways, where increased redness corresponds to greater significance (i.e., lower *p*-values).

Molecular docking

Based on a comprehensive analysis of the compound-target network, PPI network, and compound-target-disease network, the highest-ranking proteins—such as TP53, AKT1, SRC, and HSP90—were chosen for molecular docking studies. A compound (Compound 2) was docked to TP53, 11 compounds (2, 7, 11, 20, 24, 33, 38, 39, 43, 45, and 53) were docked to AKT1, 10 compounds (2, 12, 20, 27, 28, 40, 48, 49, 53, and 56) were docked to SRC, and 6 compounds (7, 12, 24, 25, 33, 55) were docked to HSP90AA1.

Table 2 showed the binding energy of the compound docked to TP53, AKT1, SRC, and HSP90AA1. Compound 2 docked to TP53 showed binding energy (-4.385 kcal/mol), higher than that of the native ligand (-6.746 kcal/mol). Molecular docking to AKT1 showed binding energies from -3.211 kcal/mol (Compound 53) to -10.005 kcal/mol (Compound 20), in which that of the AKT1 native ligand was -3.567

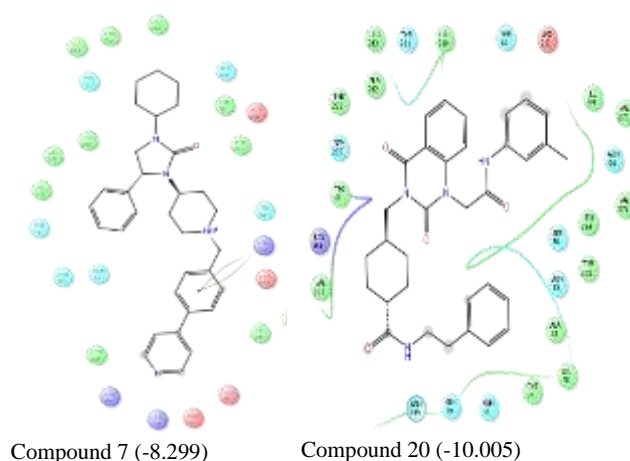
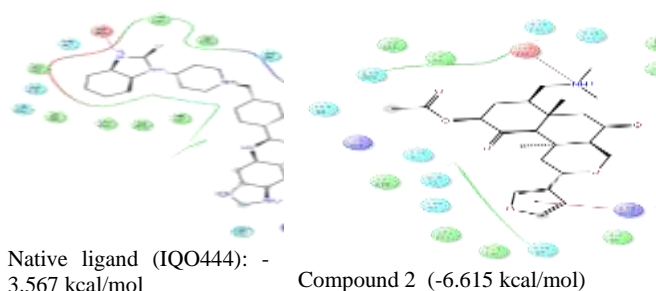
kcal/mol. Furthermore, the docking to SRC showed binding energies from -0.452 kcal/mol (Compound 49) to -5.394 kcal/mol (Compound 28), in which that of the SRC native ligand was -3.707 kcal/mol. The

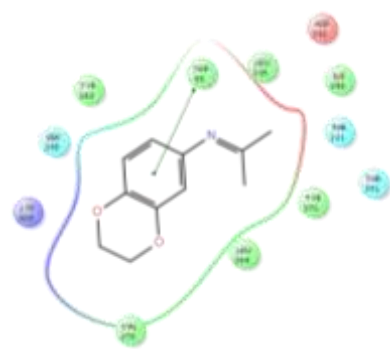
HSP90AA1 showed binding energies from -0.216 kcal/mol (Compound 33) to -10.342 kcal/mol (Compound 24), in which that of its native ligand was -5.576 kcal/mol.

Table 2: The binding energy (kcal/mol) of compound docked to TP53, AKT1, SRC, and HSP90AA1.

Compound	Binding energy (kcal/mol)			
	TP53 (PDB ID: 2VUK)	AKT1 (PDB ID: 3O96)	SRC (PDB ID: 1O43)	HSP90AA1 (PDB ID: 3O0I)
Native ligand	-6.746 (P831291)	-3.567 (IQO444)	-3.707 (821300)	-5.576 (P54237)
Compound 2	-4.385	-6.615	-2.055	
Compound 7		-8.299		-6.143
Compound 9				
Compound 11		-5.785		
Compound 12			-0.753	-2.878
Compound 20		-10.005	-1.236	
Compound 23				
Compound 24		-5.155		-10.342
Compound 25				-9.268
Compound 26				
Compound 27			-2.471	
Compound 28			-5.394	
Compound 33		-3.638		-0.216
Compound 38		-4.344		
Compound 39		-3.512		
Compound 40			-5.151	
Compound 41				
Compound 43		-6.066		
Compound 44				
Compound 45		-7.245		
Compound 48			-1.126	
Compound 49			-0.452	
Compound 50				
Compound 53		-3.211	-1.145	
Compound 55				-6.811
Compound 56			-2.471	

The molecular structures of compounds and their docking conformations to AKT1 were shown in Figure 5 and S1. Lower binding energies were observed in the AKT1-bound docked poses of Compound 2 (-6.615 kcal/mol), 7 (-8.299 kcal/mol), 11 (-5.785 kcal/mol), 20 (-10.005 kcal/mol), 24 (-5.155 kcal/mol), 33 (-3.638 kcal/mol), 38 (-4.344 kcal/mol), 43 (-6.066 kcal/mol), and 45 (-7.245 kcal/mol). In addition, higher binding energies were found in docking Compound 39 (-3.512 kcal/mol) and 53 (-3.211 kcal/mol) to AKT1.



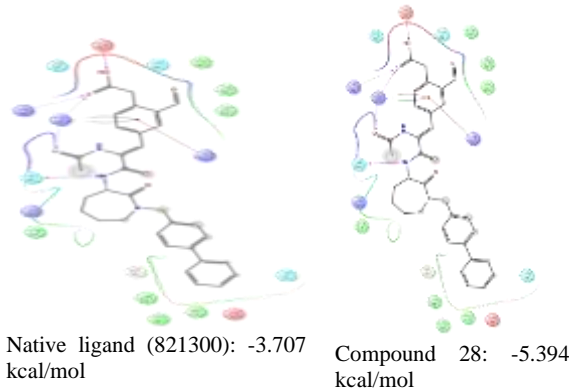


Compound 45 (-7.245)

Figure 5: The docked conformations of compounds bound to AKT1. Higher binding energies were observed in the docked poses of Compound 2 (-6.615 kcal/mol), Compound 7 (-8.299 kcal/mol), Compound 20 (-10.005 kcal/mol), and Compound 45 (-7.245 kcal/mol).

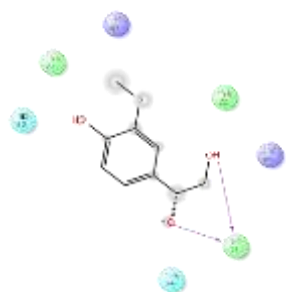
The structures of compounds and their conformation to SRC were shown in Figure 6 and S2. Lower binding energies were observed in the SRC-bound docked poses of Compound 28 (-5.394 kcal/mol) and 40 (-5.151 kcal/mol). In addition, higher binding energies were found in docking Compound 2 (-2.055 kcal/mol), 12 (-0.753 kcal/mol), 20 (-1.236 kcal/mol), 27 (-2.471 kcal/mol), 48 (-1.126 kcal/mol), 49 (-0.452 kcal/mol), 53 (-1.145 kcal/mol), and 56 (-2.471 kcal/mol) to SRC.

Figure 7 and S3 showed the structures of compounds and their docking conformation to HSP90. Lower binding energies were observed in the HSP90-docked poses of Compound 7 (-6.143 kcal/mol), 24 (-10.342 kcal/mol), 25 (-9.268 kcal/mol), and 55 (-6.811 kcal/mol). In addition, higher binding energies were found in Compound 12 (-2.878 kcal/mol) and 33 (-0.216 kcal/mol) to HSP90. Finally, molecular docking to TP53 by Compound 2 showed a binding energy of -4.385 kcal/mol, higher than that of the native ligand (-6.746 kcal/mol) (Figure S4).



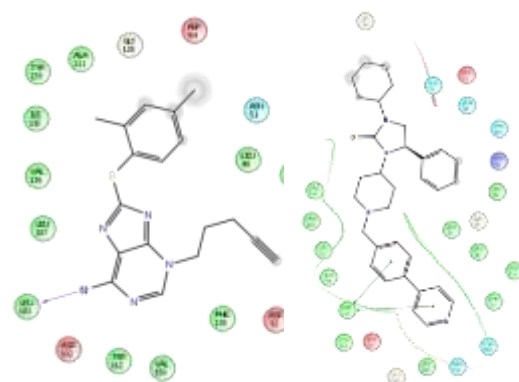
Native ligand (821300): -3.707 kcal/mol

Compound 28: -5.394 kcal/mol

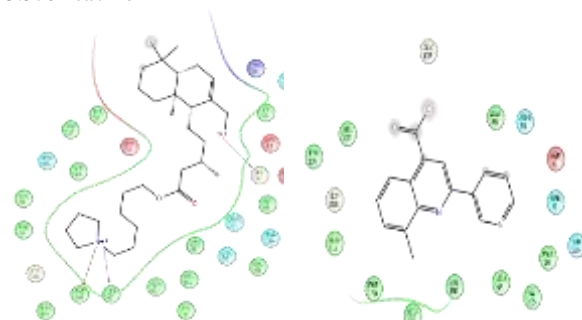


Compound 40: -5.151 kcal/mol

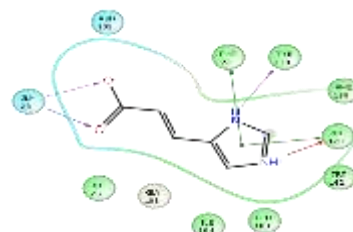
Figure 6: The docked conformations of compounds bound to SRC. Higher binding energies were observed in the docked poses of Compound 28 (-5.394 kcal/mol) and Compound 40 (-5.151 kcal/mol).



Native ligand (P54237): -5.576 kcal/mol Compound 7: -6.143 kcal/mol



Compound 24: -10.342 kcal/mol Compound 25: -9.268 kcal/mol



Compound 55: -6.811 kcal/mol

Figure 7: The docked conformations of compounds bound to HSP90. Higher binding energies were observed in the docked poses of Compound 7 (-6.143 kcal/mol), Compound 24 (-10.342 kcal/mol), Compound 25 (-9.268 kcal/mol), and Compound 55 (-6.811 kcal/mol).

In vitro anti-HCV test

In vitro anti-HCV assay of the methanol extract of *Kleinhovia hospita* L leaves was performed to get insight on antiviral effects of the extract against HCV at various concentrations. As presented in Table 3, the extract significantly inhibit HCV infection, with an IC_{50} value of $2.24 \pm 0.1 \mu\text{g/mL}$.

The network pharmacology workflow revealed tumor suppressor protein 53 (TP53), RAC-alpha serine/threonine-protein kinase (AKT1), sarcoma (SRC), heat shock protein (HSP90AA1), epidermal growth factor receptor (EGFR), glyceraldehyde-3-phosphate dehydrogenase (GAPDH), and estrogen receptor (ESR1), as key regulators. Molecular docking was performed on the top 4 protein targets, namely TP53, AKT1, SRC, and HSP90AA1. *In vitro* anti-HCV test of methanol extract of *Kleinhovia hospita* L leaves effectively inhibited HCV infection with an IC_{50} value of $2.24 \pm 0.1 \mu\text{g/mL}$. As far as the authors know, this was the first report on anti-hepatitis C inhibition of the methanol extract of *Kleinhovia hospita* L. leaves. Previous studies reported that administering a decoction of *Kleinhovia hospita* L. could stimulate liver cell regeneration and reduce the levels of SGOT and

SGPT enzymes.³⁴ Another study showed that *Kleinhovia hospita*, contained in polyherbal medicine, along with *Curcuma xanthorrhiza*, *Nigella sativa*, and *Arcangelisia flava*, provided both hepatoprotection and hepatoregeneration in CCl₄-induced chronic liver injury. The previous studies showed the anti-HCV inhibition by *Avicennia marina* leaves extract at an IC₅₀ of 12.664 ± 0.984 µg/mL.¹³ Therefore, *Kleinhovia hospita* L reported in the present study showed better inhibition toward HCV.

The potent *in vitro* inhibitory effect against HCV shown by the methanol extract of *Kleinhovia hospita* L leaves aligned with the high AKT1-binding scores of docked Compound 2, 7, 11, 20, 24, 33, 38, 43, and 45. Furthermore, there were others observed in the SRC-bound docked poses of Compounds 28 and 40, as well as those observed in the HSP90-docked poses of Compounds 7, 24, 25, and 55.

Table 3: Inhibition of Hepatitis C virus infection of *Kleinhovia hospita* L.

Concentration (µg/mL)	% of HCV inhibition	SD
100	100.00	0.00
50	100.00	0.00
10	93.90	2.11
1	19.50	3.66
0.1	0.40	0.70
0.01	0.00	0.00

Conclusion

In conclusion, this study showed that the methanol extract of *Kleinhovia hospita* L. leaves held promise in inhibiting HCV infection, as evidenced by integrated approaches including network pharmacology, molecular docking, and *in vitro* testing. Notably, compounds such as 2, 7, 11, 20, 24, 33, 38, 43, and 45 showed strong binding to AKT1. Compounds 28 and 40 showed strong binding to SRC, and well as 7, 24, 25, and 55 showed strong binding to HSP90. The extract also showed potent effects against HCV, with an IC₅₀ value of 2.24 ± 0.1 µg/mL, underscoring its therapeutic potential. These results laid the groundwork for further exploration of *Kleinhovia hospita* L. as a natural treatment candidate for HCV. Future studies will focus on the *in vivo* validation, pharmacokinetics, and safety profiling of *Kleinhovia hospita* L. methanol extract and its bioactive compounds to advance its development as a potential natural therapeutic agent against HCV.

Conflict of Interest

The author's declare no conflict of interest.

Authors' Declaration

The authors hereby declare that the work presented in this article is original and that any liability for claims relating to the content of this article will be borne by them.

Acknowledgments

The research was funded by Penelitian Fundamental Grant from Direktorat Penelitian dan Pengabdian kepada Masyarakat, Direktorat Jenderal Riset dan Pengembangan, Ministry of Higher Education, Science, and Technology Republic of Indonesia, under contract number 068/C3/DT.05.00/PL/2025.

References

- Cui F, Blach S, Manzeno Mingiedi C, Gonzalez MA, Sabry Alaama A, Mozalevskis A, Séguy N, Rewari BB, Chan P-L, Le L-v, Doherty M, Luhmann N, Easterbrook P, Dirac M, de Martel C, Nayagam S, Hallett TB, Vickerman P, Razavi H, Lesi O, Low-beer D. Global reporting of progress towards elimination of hepatitis B and hepatitis C. *Lancet Gastroenterol. Hepatol.* 2023;8(4):332-342.
- Yang C, Lv F, Yang J, Ding D, Cui L, Han Y. Surveillance and management of hepatocellular carcinoma after treatment of hepatitis C with direct-acting antiviral drugs. *Ann. Hepatol.* 2025;30(2):101582.
- Devarbhavi H, Asrani SK, Arab JP, Narthey YA, Pose E, Kamath PS. Global burden of liver disease: 2023 update. *J. Hepatol.* 2023;79(2):516-537.
- Wasityastuti W, Nugrahaningsih D, Ratnoglik S, Yamani L, Aoki-Utsubo C, Wahyuni T. *In vitro* Immunomodulatory and Hepatoprotective Activities of Selected Indonesian Medicinal Plants. *Trop. J. Nat. Prod. Res.* 2025;9(5):2329 - 2334.
- Omari HEL, El-Mouhdi K, Ouarrak K, Talbi FZ, Mesbah F, Milouk FZ, Dahmani F, Lhilali I, Amrani JE, Lalami AE. Impact of Rainfall on The Distribution of Water-Borne Diseases: The Case of Viral Hepatitis. *Trop. J. Nat. Prod. Res.* 2023;7(6):3136-3139.
- Arung ET, Kusuma IW, Purwatiningsih S, Roh S-S, Yang CH, Jeon S, Kim Y-U, Sukaton E, Susilo J, Astuti Y, Wicaksono BD, Sandra F, Shimizu K, Kondo R. Antioxidant Activity and Cytotoxicity of the Traditional Indonesian Medicine Tahongai (*Kleinhovia hospita* L.) Extract. *J. Acupunct. Meridian Stud.* 2009;2(4):306-308.
- Ariefita NR, Sofian FF, Aboshi T, Kuncoro H, Dinata DI, Shiono Y, Nishikawa Y. Evaluation of the antiplasmodial and anti-Toxoplasma activities of several Indonesian medicinal plant extracts. *J. Ethnopharmacol.* 2024;331:118269.
- Solihah I, Herlina H, Rasyid RSP, Suciati T, Khairunnisa K. A Cytotoxic Activity of Tahongai (*Kleinhovia hospita* Linn.) Leaves Extracts Using Brine Shrimp Lethality Test. *Sci. Technol. Indones.* 2019;4(3):60-63.
- Zubair MS, Yuyun Y, Musnina WS, Najib A, Nainu F, Arba M, Paneo DR, Praditapuspita EN, S. M. Network Pharmacology and Molecular Docking Studies of Ethnopharmacological Plants from Sulawesi as Antidiabetics. *Trop. J. Nat. Prod. Res.* 2025;9(3):1123 -1135.
- Fitrianingsih AA, Santosaningsih D, Djajalaksana S, Muti, ah R, Lusida MI, Karyono SS, Prawiro SR. Network Pharmacology and *In Silico* Investigation on *Saussurea lappa* for Viral Respiratory Diseases. *Trop. J. Nat. Prod. Res.* 2024;8(1):5889-5896.
- Murdiana HE, Murwanti R, Fakhruddin N, Ikawati Z. Multi-target mechanism of polyherbal extract to treat diabetic foot ulcer based on network pharmacology and molecular docking. *J. Herbmed Pharmacol.* 2024;13(2):289-299.
- Zubair MS, Maulana S, Widodo A, Pitopang R, Arba M, Hariono M. GC-MS, LC-MS/MS, docking and molecular dynamics approaches to identify potential SARS-CoV-2 3-chymotrypsin-like protease inhibitors from *Zingiber officinale* Roscoe. *Molecules.* 2021;26(17):5230.
- Arba M, Ihsan S, Hatma FMI, Jamili J, Wahyudi ST, TS W. Inhibition of hepatitis C virus by *Avicennia marina* (Forssk.) Vierh. leaves extract: Liquid chromatography-high-resolution mass spectrometry, network pharmacology, molecular simulation, and *in vitro* study. *J. Herbmed Pharmacol.* 2025;14(2):188-199.
- Windarsih A, Suratno, Warmiko HD, Indrianingsih AW, Rohman A, Ulumuddin YI. Untargeted metabolomics and proteomics approach using liquid chromatography-Orbitrap high resolution mass spectrometry to detect pork adulteration

- in *Pangasius hypophthalmus* meat. Food Chem. 2022;386:132856.
15. Daina A, Michielin O, Zoete V. SwissADME: a free web tool to evaluate pharmacokinetics, drug-likeness and medicinal chemistry friendliness of small molecules. Sci. Rep. 2017;7(1):42717.
 16. Daina A, Michielin O, Zoete V. SwissTargetPrediction: updated data and new features for efficient prediction of protein targets of small molecules. Nucleic Acids Res. 2019;47(W1):W357-W364.
 17. Keiser MJ, Roth BL, Armbruster BN, Ernsberger P, Irwin JJ, Shoichet BK. Relating protein pharmacology by ligand chemistry. Nat. Biotechnol. 2007;25(2):197-206.
 18. Rebhan M, Chalifa-Caspi V, Prilusky J, Lancet D. GeneCards: a novel functional genomics compendium with automated data mining and query reformulation support. Bioinformatics. 1998;14(8):656-664.
 19. Amberger JS, Bocchini CA, Schiettecatte F, Scott AF, Hamosh A. OMIM.org: Online Mendelian Inheritance in Man (OMIM®), an online catalog of human genes and genetic disorders. Nucleic Acids Res. 2015;43(D1):D789-D798.
 20. Arba M, Ihsan S, Fatihah N, Jamili J. Molecular Mechanism of *Avicennia marina* (Forssk.) Vierh. in Inhibiting Hepatitis C Virus Based on Network Pharmacology and Molecular Docking. Trop. J. Nat. Prod. Res. 2025;9(4):1449 – 1456.
 21. Jiang L-R, Qin Y, Nong J-L, An H. Network pharmacology analysis of pharmacological mechanisms underlying the anti-type 2 diabetes mellitus effect of guava leaf. Arab J. Chem. 2021;14(6):103143.
 22. Shannon P, Markiel A, Ozier O, Baliga NS, Wang JT, Ramage D, Amin N, Schwikowski B, Ideker T. Cytoscape: A Software Environment for Integrated Models of Biomolecular Interaction Networks. Genome Res. 2003;13(11):2498-2504.
 23. Kanehisa M, Furumichi M, Tanabe M, Sato Y, Morishima K. KEGG: new perspectives on genomes, pathways, diseases and drugs. Nucleic Acids Res. 2017;45(D1):D353-D361.
 24. Zhou Y, Zhou B, Pache L, Chang M, Khodabakhshi AH, Tanaseichuk O, Benner C, Chanda SK. Metascape provides a biologist-oriented resource for the analysis of systems-level datasets. Nat. Commun. 2019;10(1):1523.
 25. Ge SX, Jung D, Yao R. ShinyGO: a graphical gene-set enrichment tool for animals and plants. Bioinformatics. 2020;36(8):2628-2629.
 26. Arba M, Ruslin, Ihsan S, Tri Wahyudi S, Tjahjono DH. Molecular modeling of cationic porphyrin-anthraquinone hybrids as DNA topoisomerase II β inhibitors. Comput. Biol. Chem. 2017;71:129-135.
 27. Citra SNAL, Arfan A, Alroem A, Bande LS, Irnawati I, M A. Docking-based workflow and ADME prediction of some compounds in *Curcuma longa* and *Andrographis paniculata* as polymerase PA-PB1 inhibitors of influenza A/H5N1 virus. J. Res. Pharm. 2023;27(1):221-231.
 28. Arba M, Paradis N, Wahyudi ST, Brunt DJ, Hausman KR, Lakernick PM, Singh M, Wu C. Unraveling the binding mechanism of the active form of Remdesivir to RdRp of SARS-CoV-2 and designing new potential analogues: Insights from molecular dynamics simulations. Chem. Phys. Lett. 2022;799:139638.
 29. Sastry GM, Adzhigirey M, Day T, Annabhimoju R, Sherman W. Protein and ligand preparation: parameters, protocols, and influence on virtual screening enrichments. J. Comput. Aided Mol. Des. 2013;27(3):221-234.
 30. Wahyuni TS, permatasari AA, Widiandani T, Fuad A, Widyawaruyanti A, Aoki-Utsubo C, Hotta H. Antiviral Activities of Curcuma Genus against Hepatitis C Virus. Nat. Prod. Commun. 2018;13(12):1579-1582.
 31. Apriyanto DR, Aoki C, Hartati S, Hanafi M, Kardono LBS, Arsianti A, Louisa M, Sudiro TM, Dewi BE, Sudarmono P, Soebandrio A, Hotta H. Anti-Hepatitis C Virus Activity of a Crude Extract from Longan (*Dimocarpus longan* Lour.) Leaves. Jpn. J. Infect. Dis. 2016;69(3):213-220.
 32. Widyawaruyanti A, Tanjung M, Permanasari AA, Saputri R, Tumewu L, Adianti M, Aoki-Utsubo C, Hotta H, Hafid AF, Wahyuni TS. Alkaloid and benzopyran compounds of *Melicope latifolia* fruit exhibit anti-hepatitis C virus activities. BMC Complement Med Ther. 2021;21(1):27.
 33. Zhou W, Wang Y, Lu A, Zhang G. Systems pharmacology in small molecular drug discovery. Int. J. Mol. Sci. 2016;17(2):246.
 34. Saranani M, Nurfantri N. The Effectiveness of Tawandakulo (*Kleinhovia hospita* L.) On SGOT, SGPT Enzyme Levels, and Hepatocyte Regeneration in Paracetamol-Induced Rats. Public Health Indones. 2024;10(3):373 - 382.